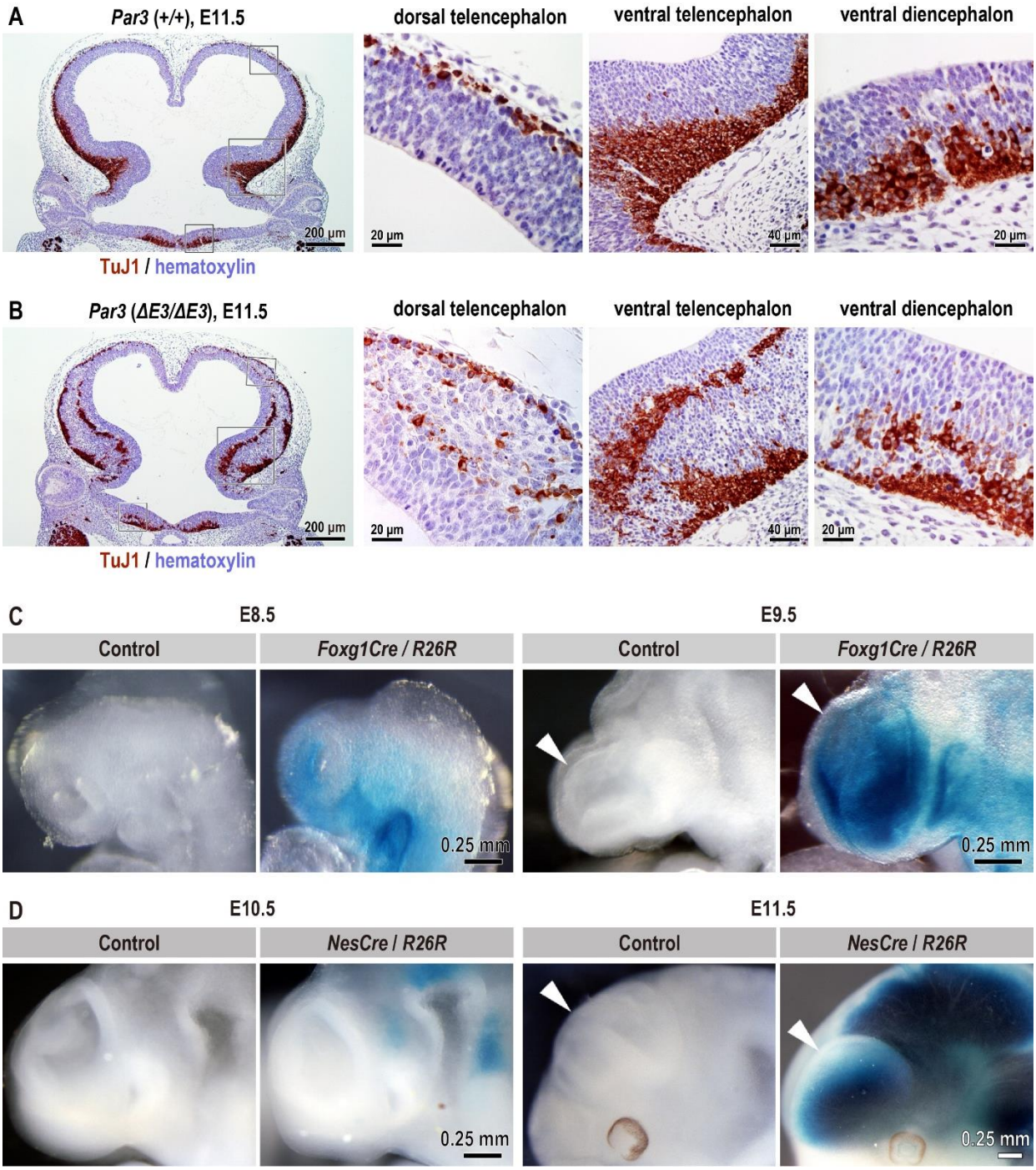

Fig. S1. Disturbed neural tissue development in the forebrain of *Par3*$^{\Delta/\Delta}$ embryos and developmental stage-dependent recombination of the *Rosa26R* allele mediated by *Foxg1-Cre* or *Nestin-Cre*.

(A, B) Immunohistochemistry of TuJ1 in coronal sections of the forebrain of control and survived *Par3*$^{\Delta/\Delta}$ embryos at E11.5. Squares correspond to the regions magnified alongside. X-gal staining of the heads of *Foxg1-Cre*;*Rosa26R* (C), *Nestin-Cre*;*Rosa26R* (D), and corresponding control embryos. Arrowheads indicate the telencephalic vesicle.

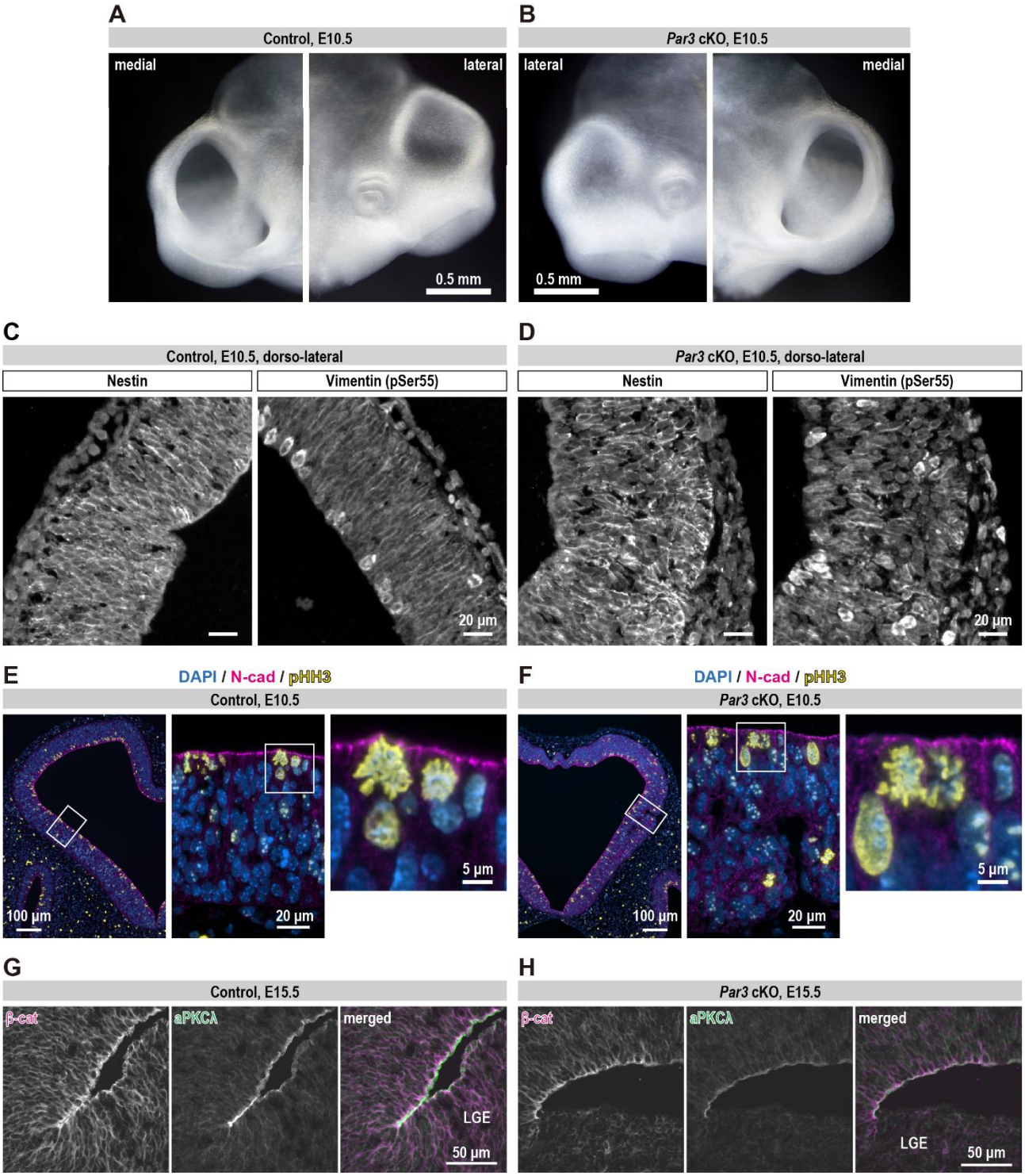

Fig. S2. Disorganized morphology and cell-cell junctions of *Par3* cKO NPCs at early and later developmental stages, respectively.

(A, B) Gross appearance of sagittally dissected control and *Par3* cKO heads. (C, D) Immunofluorescence of Nestin and p-Vimentin in control and *Par3* cKO telencephalons at E10.5. (E–H) Immunofluorescence of the marker proteins of cell-cell junctions (N-cadherin, N-cad; β-catenin, β-cat), dividing cells (phospho-Histone H3, pHH3), and apical domains (aPKCλ) in control and *Par3* cKO telencephalons at E10.5 (E, F) and E15.5 (G, H). Rectangles correspond to the regions magnified alongside.

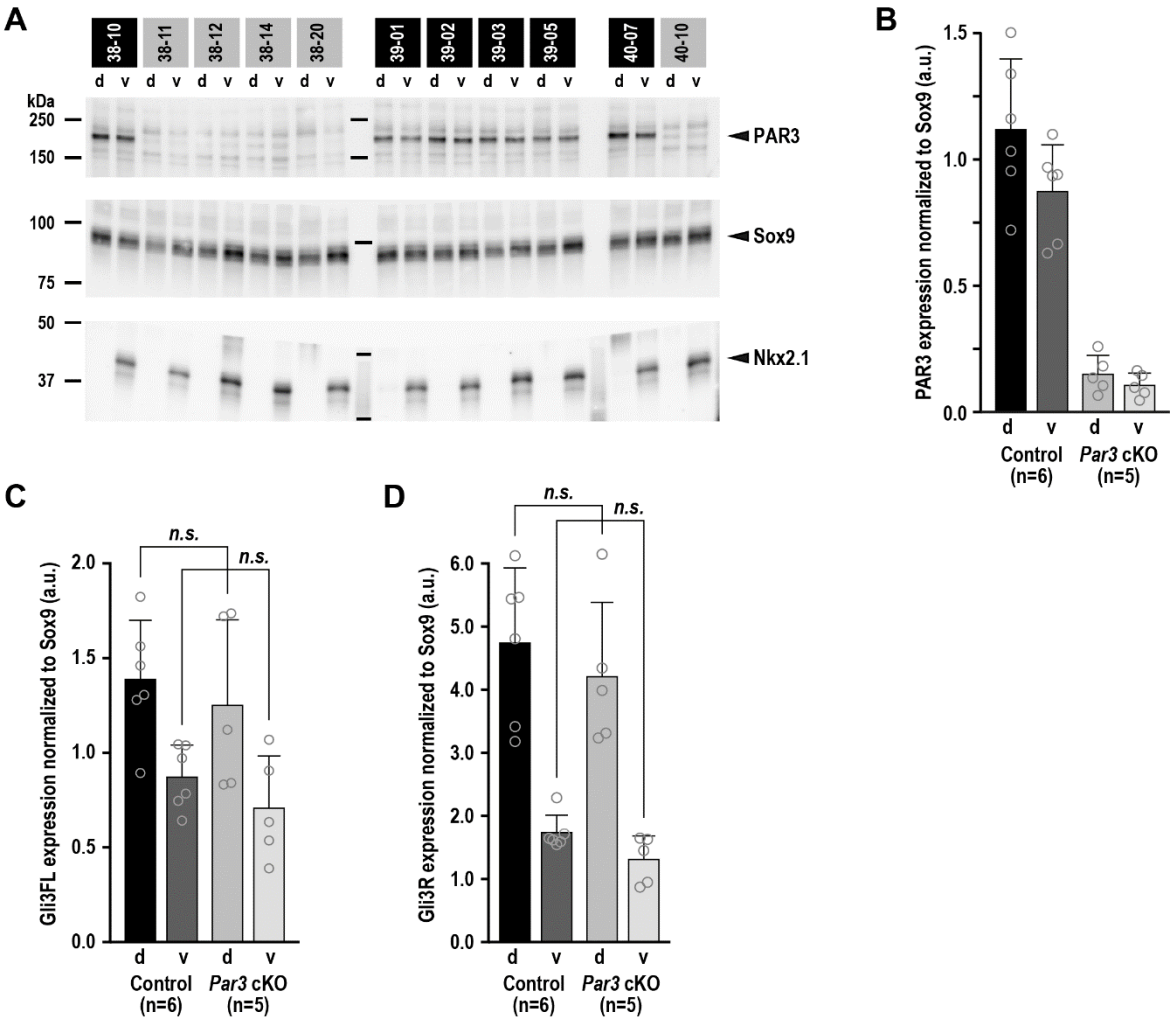

Fig. S3. Protein extracts were successfully prepared from dorsal and ventral telencephalons at E11.5.

(A) Immunoblot analysis of the indicated proteins in separately dissected dorsal (d) and ventral (v) telencephalons at E11.5. Sox9 and Nkx2.1 were used as loading controls for NPCs and the ventral telencephalon, respectively. The IDs of control and *Par3* cKO embryos are labeled in white and black, respectively. The genotypes of control embryos are *Foxg1*$^{+/Cre}$;*Par3*$^{floxE3/+}$ (38-10, 40-7) or *Foxg1*$^{+/Cre}$;*Par3*$^{\Delta E3/+}$ (39-01, 39-02, 39-03, 39-05). (B–D) Quantification of the expressions of PAR3 (B), Gli3FL (C; Fig. 5E), and Gli3R (D; Fig. 5E) normalized to Sox9, respectively.

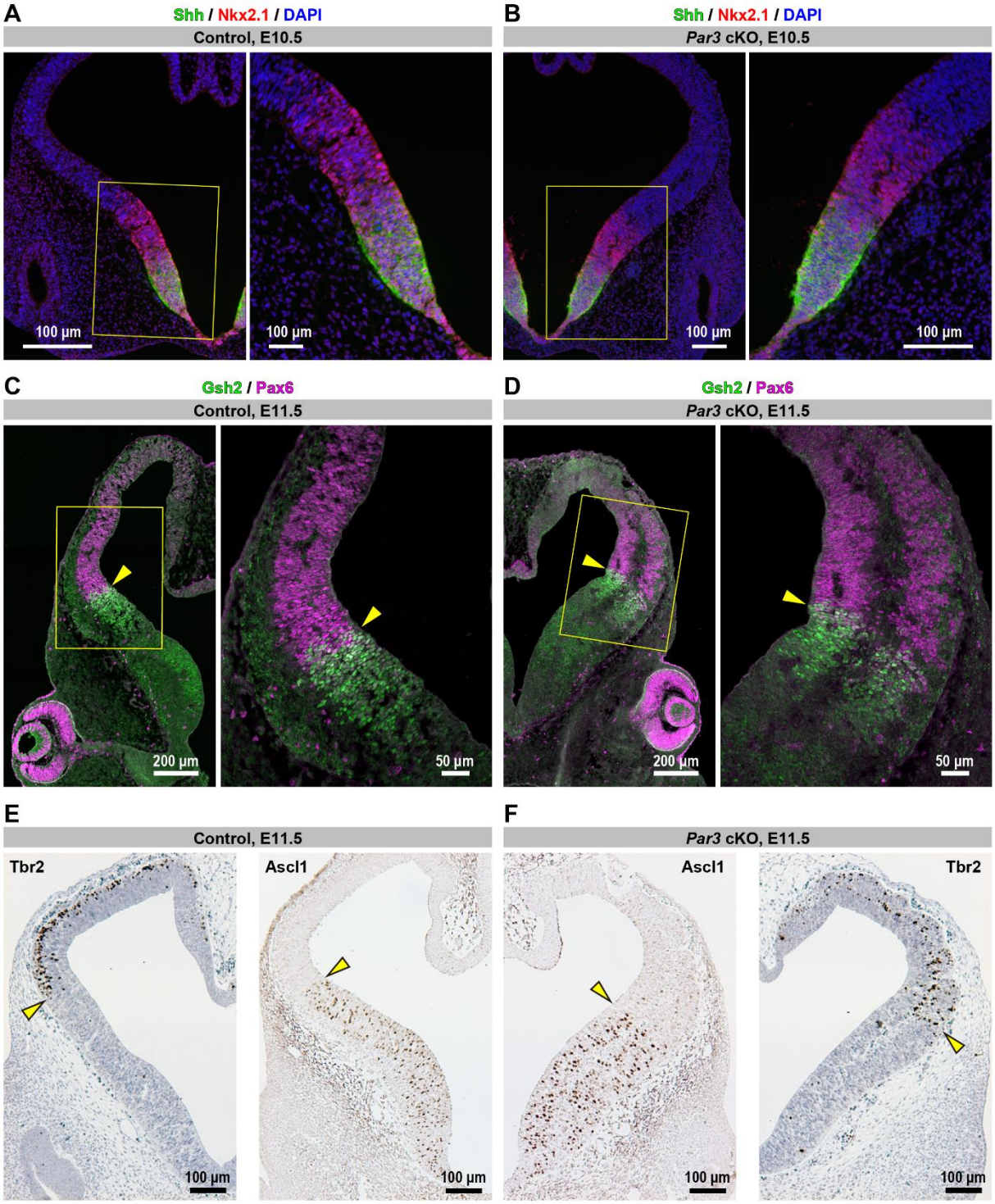

Fig. S4. Expression of Shh and dorsoventral patterning are not compromised in the *Par3* cKO telencephalon.

(A–F) Immunofluorescence or immunohistochemistry of the indicated targets in the coronal sections of control and *Par3* cKO telencephalons at E10.5 (A, B) or E11.5 (C–F). Ectopic NPCs in *Par3* telencephalons express all the stem or progenitor markers examined, showing proliferative activity with preserved differentiation potential as well as dorsoventral characteristics. Rectangles correspond to the regions magnified alongside. Arrowheads indicate the pallial-subpallial boundaries.

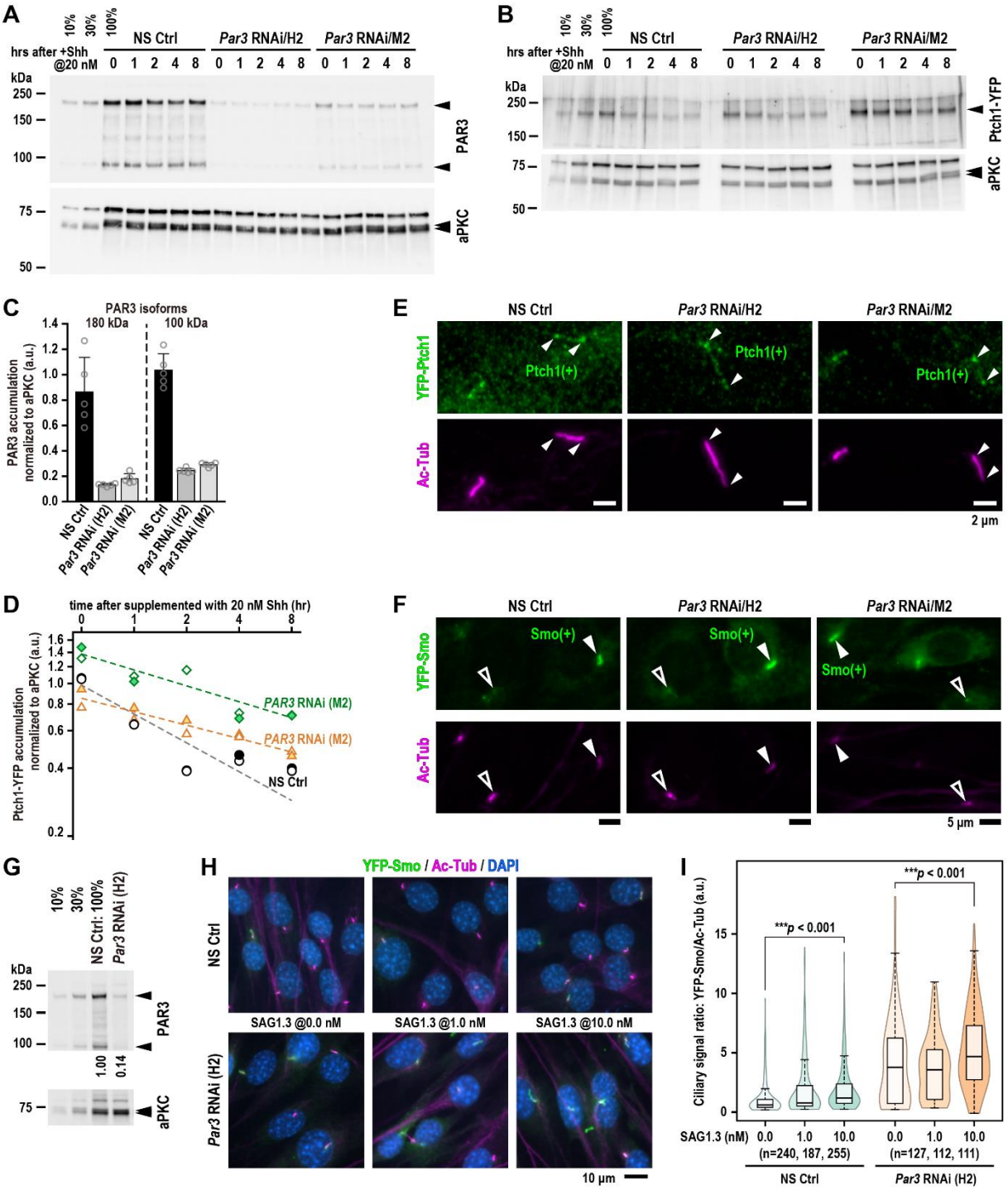

Fig. S5. Flp-In-3T3/Ptch1-YFP and Flp-In-3T3/YFP-Smo cells preserve responses to Shh or SAG1.3 with reduced PAR3 expression.

(A–D) Representative immunoblot analysis of the indicated proteins in Flp-In-3T3/Ptch1-YFP cells transfected with the indicated siRNAs and stimulated with recombinant Shh (C24II) at 20 nM for 0 to 8 h. (D) The time course of the Shh-induced degradation of Ptch1-YFP. (E, F) Higher magnification images of immunofluorescence shown in Fig. 6G, I. (G) Immunoblot analysis of the indicated proteins in Flp-In-3T3/YFP-Smo cells transfected with the indicated siRNAs. The values below the bands show the relative intensities of PAR3 normalized to aPKC. (H) Representative immunofluorescence of YFP and acetylated-tubulin (Ac-Tub), and DAPI staining in Flp-In-3T3/YFP-Smo cells transfected with the indicated siRNAs followed by serum starvation and stimulation by SAG1.3 at 0 to 10 nM for 19 h. (I) Quantification of ciliary accumulated YFP-Smo. The p-values were determined using the Brunner–Munzel test.

Table S1. Mouse strains used in this study

Mouse strain	Reference / Supplier	Identifier
Par3$^{\Delta E3}$ (*Pard3*$^{tm1.1Shoh}$)	(Hirose et al., 2006)	MGI Cat# 3838017; RRID: MGI: 3838017
Par3^{floxE3}	(Iden et al., 2012)	N/A
Foxg1-Cre (129(Cg)-*Foxg1*$^{tm1(cre)Skm}$/J)	(Hébert and McConnell, 2000)	IMSR Cat# JAX: 004337; RRID: IMSR_JAX:004337
129X1/SvJ	The Jackson Laboratory, Bar Harbor, ME	IMSR Cat# JAX: 000691; RRID: IMSR_JAX:000691
C57BL/6JJcl	CLEA Japan, Inc., Tokyo, Japan	RRID:IMSR_JCL:JCL:mIN-0003
Nestin-Cre	(Imai et al., 2006)	N/A
ROSA26 (*Gt(ROSA)26Sor*^{tm1Sor})	The Jackson Laboratory (Soriano, 1999)	IMSR Cat# JAX:003309; RRID: IMSR_JAX:003309

Table S2. Antibodies used in this study. Suppliers and identifiers for the primary and secondary antibodies used.

Click here to download Table S2

Table S3. Oligonucleotides used in this study. PCR primers and probes used for genotyping and TaqMan gene expression assays.

Click here to download Table S3

Table S4. Software and packages used for data acquisition and analyses.

Software and package	Supplier	Identifier
Multi Gauge	Fujifilm, Tokyo, Japan	RRID: SCR_014299 Ver. 2.2
iQ5 Optical System Software	Bio-Rad, Tokyo, Japan	Ver. 2.0
Huygens Professional	Scientific Volume Imaging, Hilversum, Netherlands	RRID: SCR_014237 Ver. 17.10.0p8 64b (Jul. 30, 2018)
ImageJ	(Schneider et al., 2012)	RRID: SCR_003070 https://imagej.nih.gov/ij/
R statistical software	R Foundation for Statistical Computing (R Core Team, 2020)	RRID: SCR_001905 https://www.R-project.org/
RStudio Desktop	RStudio, Inc.	Version 1.2.5033
R package, brunnermunzel: (Permuted) Brunner-Munzel Test	Toshiaki Ara	R package version 1.4.1. https://CRAN.R-project.org/web/packages/brunnermunzel/
R package, beeswarm: The Bee Swarm Plot, an Alternative to Stripchart	Aron Eklund and James Trimble	R package version 0.4.0. https://CRAN.R-project.org/web/packages/beeswarm/
R package, vioplot: Violin Plot	S. Thomas Kelly, Daniel Adler, and Tom M. Elliott	R package version 0.3.7 https://CRAN.R-project.org/web/packages/vioplot/
R package, RColorBrewer: ColorBrewer Palettes	Erich Neuwirth	R package version 1.1-3 https://CRAN.R-project.org/web/packages/RColorBrewer/

Supplementary References

Hébert, J. M. and McConnell, S. K. (2000). Targeting of cre to the Foxg1 (BF-1) Locus Mediates loxP Recombination in the Telencephalon and Other Developing Head Structures. *Dev. Biol.* **222**, 296–306.

Hirose, T., Karasawa, M., Sugitani, Y., Fujisawa, M., Akimoto, K., Ohno, S. and Noda, T. (2006). PAR3 is essential for cyst-mediated epicardial development by establishing apical cortical domains. *Development* **133**, 1389–1398.

Iden, S., van Riel, W. E., Schafer, R., Song, J. Y., Hirose, T., Ohno, S. and Collard, J. G. (2012). Tumor type-dependent function of the par3 polarity protein in skin tumorigenesis. *Cancer Cell* **22**, 389–403.

Imai, F., Hirai, S., Akimoto, K., Koyama, H., Miyata, T., Ogawa, M., Noguchi, S., Sasaoka, T., Noda, T. and Ohno, S. (2006). Inactivation of aPKCλ results in the loss of adherens junctions in neuroepithelial cells without affecting neurogenesis in mouse neocortex. *Development* **133**, 1735–44.

R Core Team (2020). R: A language and environment for statistical computing. R Foundation for Statistical Computing, Vienna, Austria. (https://www.R-project.org/). *https://www.R-project.org/*.

Schneider, C. A., Rasband, W. S. and Eliceiri, K. W. (2012). NIH Image to ImageJ: 25 years of image analysis. *Nat. Methods* **9**, 671–675.

Soriano, P. (1999). Generalized lacZ expression with the ROSA26 Cre reporter strain. *Nat. Genet.* **21**, 70–71.